Pulsed NMR in Extracting Spin-Spin and Spin-Lattice Relaxation Times of Mineral Oil and Glycerol

Kent Lee, Dean Henze, Patrick Smith, and Janet Chao
University of San Diego
(Dated: February 24, 2013)

Using TeachSpin's PS1-A nuclear magnetic resonance (NMR) spectrometer, we preformed inversion recovery and spin echo experiments on samples of both glycerol and mineral oil with the goal of determining spin-lattice and spin-spin relaxation times, T_1 and T_2. In glycerol, T_1 was found to be 42.6 ms with a relative uncertainty of 1.7% while T_2 was found to be 47.4 ms with a relative uncertainty of 9.5%. In mineral oil, T_1 was found to be 20.9 ms with a relative uncertainty of 3.4% while T_2 was found to be 21.2 ms with a relative uncertainty of 11.8%.

I. INTRODUCTION

Since Bloch and Purcell's discovery of nuclear magnetic resonance (NMR) in 1946, interest blossomed in the field of NMR theory and application. Improved understanding and accelerated development in the field of NMR has made it invaluable not only in the field of physics, but also in the fields of chemistry and medicine. From helping to understand the classical and quantum properties of nuclei to chemical structure analysis to soft-tissue imaging, this form of non-invasive, non-destructive technology has contributed to the furthering of countless studies. In fact, the impact of NMR discovery is so significant that it is a widely taught subject both in undergraduate and graduate courses.

In teaching NMR theory, it is important to not only explain the theory, but also show experimental applications of the theory in an actual spectrometer to promote a thorough understanding of NMR theory. As such, TeachSpin has developed several NMR instruments designed for teaching NMR spectroscopy and NMR theory. It is through one of TeachSpin's products that the following exploration of NMR spin-spin and spin-lattice relaxation times was conducted. The goal was to learn more about NMR theory by applying it to two sample liquids, glycerol and mineral oil. Specifically, both spin-spin and spin-lattice relaxation times for both glycerol and mineral oil were determined.

The theory behind NMR will first be discussed both from a quantum mechanical perspective and classically. Once the theory of spin-lattice and spin-spin relaxation time is explained, the experimental design used to determine the relaxation times will be introduced. The results of the experiment will then be presented, followed by a discussion of the results.

II. THEORY

A. Quantum Interpretation

Protons and neutrons, the substituents of the nucleus of an atom, are much like electrons in that they are both particles with spin $\frac{1}{2}$, represented as $I = \frac{1}{2}$, both reside in discrete energy levels, and both have magnetic moments. Because the nucleus is composed of protons and neutrons, the nucleus also has angular momentum and a magnetic moment. In a given nucleus with angular momentum $\mathbf{I}$ and magnetic moment $\boldsymbol{\mu}$ aligned along the spin axis, there is a proportionality that exists, given by

$$\boldsymbol{\mu} = \gamma\hbar\mathbf{I}, \tag{1}$$

where γ is known as the gyromagnetic ratio, with dimensions of radians per second-tesla. For a proton, $\gamma = 2.675 \times 10^8\ \mathrm{s^{-1}T^{-1}}$.

For a given nucleus of total spin I, it can exist in any of the $(2I+1)$ sublevels m_I, where $m_I = (I, I-1, I-2, ...)$. In the absence of a magnetic field, these sublevels are degenerate. However, when the nucleus is placed in a magnetic field B_0, the energies of these sublevels become different, with the energies of each sublevel being given by

$$\frac{E}{\hbar} = -\gamma B_0 m_I, \tag{2}$$

with the energy difference between adjacent energy sublevels, where $\Delta m_I = \pm 1$, being given by

$$\frac{\Delta E}{\hbar} = \gamma B_0 = \omega_0, \tag{3}$$

where ω_0 is known as the Larmor frequency.

For simplicity, the case of a proton is considered (as in the ion H^+, where the nucleus is simply a proton). The spin of a proton is $\frac{1}{2}$, so the total nuclear spin (I) is $I = \frac{1}{2}$ and there are only two sublevels, $m_I = -\frac{1}{2}$ and $m_I = +\frac{1}{2}$. In the absense of a magnetic field B_0, the two sublevels are degenerate. When a B_0 is applied to the proton, the sublevels split in energy, with the state with spin parallel to B_0 being lower in energy. Thus, defining $+z$ by the direction of B_0, $m_I = +\frac{1}{2}$ is the lower energy state. Given a population of protons in thermal equilibirum, the population distribution in the lower energy spin up state $(m_I = +\frac{1}{2})$ will be greater than the population distribution in the higher energy spin down state $(m_I = -\frac{1}{2})$ because of the Boltzmann distribution

$$N(E) = N_0 e^{-E/kT}, \tag{4}$$

where $N(E)$ is the number of particles in energy state E, N_0 is the normalization factor, T is the temperature in Kelvins, and k is the Boltzmann constant [1].

In summary, when a population of protons are at thermal equilibrium in the presence of a magnetic field, the lower energy, spin up state will have a higher population than the higher energy spin down state; the equations of each state are time independent. However, it can be shown by time-dependent perturbation theory that, by applying a perturbing magnetic field $H_1 \ll B_0$ rotating at frequency equal to the Larmor frequency of the sample, the probability to be in each state becomes dependent on the length of time that H_1 is applied. Thus, by applying a rotating field H_1 at the same frequency as the energy difference between the two states, the probability in each state vary in a time dependent manner and are predictable. At a time equal to $\pi/2$ of a cycle of time dependent wavefunction, the probability of being in the spin up state is equal to the probability of being in the spin down state; the two states are superposed. As seen in the Stern-Gerlach experiment, probing a superimposed state yields polarization onto an orthogonal axis. Thus, since the spin states are in the z axis (due to the static magnetic field in the z axis), the superimposed states become polarized onto the $+x$ axis, which is the basis of the $\pi/2$ pulse discussed later.

Therefore, in a nucleus with nonzero angular momentum (I) and nonzero magnetic moment ($\boldsymbol{\mu}$), the simultaneous presence of a static magnetic field B_0 and a perturbing magnetic field H_1 operating at the Larmor frequency yields equally populated spin states if applied for the proper duration of time. Because H_1 rotates at the Larmor frequency, it is able to promote spins from one state to another, given that the energy difference is the Larmor frequency. Once the presence of H_1 is removed, however, the population of the states will decay back to that of thermal equilibrium, with higher population in the lower energy state.

B. Classical Interpretation

As discussed above, in thermal equilibrium within a magnetic field, a population of protons will have an unequal distribution of spin states, with a higher population of protons being in the spin up state than the spin down state, as demonstrated by Eq. 4. This leads to a net magnetization in the proton population when placed in a static magnetic field, where net magnetic alignment parallel to the magnetic field, in the $+z$ direction, is achieved.

Classically, nuclei with nonzero spin can be considered to be a small bar magnet with magnetic moment $\boldsymbol{\mu}$ rotating and angular momentum vector $\mathbf{J}$. If a constant magnetic field B_0 is applied along the z axis, B_0 will apply a torque on the magnetic moment, leading to $\mathbf{J}$ precessing around the z axis with an angular frequency ω_0 given by

$$\omega_0 = \gamma B_0, \tag{5}$$

which is also known as the Larmor frequency (which is the same as Eq. 3, which describes the frequency required for transition between adjacent sublevels, but derived from two different phenomenon), with the precession being known as the Larmor precession.

When a magnetic field $\mathbf{H}_1$ orthogonal to and much weaker than the static magnetic field rotating around the z axis at an angular frequency ω is used, the nuclear magnetic dipole is torqued. When $\omega = \omega_0$, a productive, non-cancelling torque is applied to the nuclear magnetic dipole, increasing the angle θ between the precessing magnetic moment's spin axis and B_0. Since the energy of the nucleus in a magnetic field is

$$E = -\boldsymbol{\mu} \cdot \mathbf{B}_0 = -\gamma \hbar I B_0 \cos\theta, \tag{6}$$

this change in θ due to $\mathbf{H}_1$ causes a change in the energy of the nucleus, which is analagous to the transitions between sublevels explained in Sec. II A, the section about the quantum interpretation. Furthermore, if the system is observed from a rotating frame of reference around the z axis at an angular frequency of ω_0, $\mathbf{J}$ will appear to precess around $\mathbf{H}_1$ with a frequency of $\omega = \gamma H_1$ due to Larmor precession. If $\mathbf{H}_1$ is administered for just the right duration of time (known as a $\pi/2$ pulse because it is a quarter of the cycle), the dipole is torqued just enough to begin to precessing in the xy plane, an event which can be observed if there is a coil receiver aligned with the x axis. This precession in the xy plane can be seen as a superposition of both spin up and spin down states and is analagous to the equally populated states in the quantum discussion above.

C. $\pi/2$ and π Pulses

The previous two subsections have asserted that the probability to be in each state (spin up or spin down) is time independent when nuclei are in a static magnetic field B_0. However, when a perturbing magnetic field H_1 is applied, the probability to be in each state becomes time dependent. Thus, for a given length of time that H_1 is applied, the probabilies to be in each state are known. Two important pulse lengths (given as proportions of the magnetic field's frequency) are $\pi/2$ and π because at these lengths of time, the population in the two states are equal and inverted, respectively. Thus, applying a $\pi/2$ pulse (applying H_1 for an amount of time equal to $\pi/2$ of the cycle) will cause the two populations to shift from the equilibrium distribution of higher population in spin

up state to having equal populations in both states. Similarly, applying a π pulse will cause the two populations to shift from spin up state having a higher population to the spin down state having a higher population. The actual length of time for a given H_1 at frequency ω to achieve a $\pi/2$ and a π pulse are, respectively,

$$t_{\frac{\pi}{2}} = \frac{\frac{\pi}{2}}{\omega} \text{ and } t_\pi = \frac{\pi}{\omega}. \tag{7}$$

D. T_1 and Spin-Lattice Relaxation

When a sample of nuclei are examined in absence of any magnetic field, the population of each state should be equal because the two states are degenerate. The magnetization of a sample is given by

$$M_z = (N_1 - N_2)\mu, \tag{8}$$

where N_1 and N_2 are the population in each of the states. Thus in the absence of a magnetic field, the magnetization should be zero. However, when placed in a static magnetic field, magnetization of the sample occurs because the two states are now different in energy, which, as predicted by Eq. 4, will lead to a higher population in the lower energy state. Since $N_1 \neq N_2$, there is a net magnetization. However, this net magnetization when the sample is placed in a static magnetic field is not instantaneous; a finite time is required for the population to reach equilibrium within B_0. This magnetization process can be described by

$$\frac{dM_z}{dt} = -\frac{M_0 - M_z}{T_1}, \tag{9}$$

where M_0 is the magnetization as time goes to infinity and T_1 is the characteristic time scale for reaching M_0. Thus, T_1 yields an idea of the amount of time it takes for magnetization from an unmagnetized sample. T_1 is unique for each sample and typically ranges from microseconds to seconds. T_1 is also known as the spin-lattice relaxation time because when going from equal population in both state to higher population in the lower energy state, energy is released from the nuclei to the surrounding, which is also known as the lattice. The time it takes for this energy exchange from the nuclei to the lattice contributes to why magnetization is not instantaneous. The study of what causes different samples to have different T_1 is a major topic in magnetic resonance.

E. T_2 and Spin-Spin Relaxation

Also of interest is the amount of time it takes to reach equilibrium on the transverse plane. That is, how long would it take B_0 to reduce magnetization from being only in one direction in the xy plane to being in every direction in the xy plane, and thus, equilibrium. One could imagine if a $\pi/2$ pulse was administered after a sample has been in thermal equilibrium within B_0, the magnetization would then move from being on $+z$ axis to $+x$ axis. The question, then, is what is the time scale that it takes to cause magnetization in the $+x$ axis to decay. This process is governed by the differential equations

$$\frac{dM_x}{dt} = -\frac{M_x}{T_2} \text{ and } \frac{dM_y}{dt} = -\frac{M_y}{T_2}, \tag{10}$$

where M_x and M_y are the x and y components of the transverse magnetization and T_2 is the characteristic relaxation time for spin-spin relaxation [2]. The solutions to these equations are

$$M_x(t) = M_0 e^{-\frac{t}{T_2}} \text{ and } M_y(t) = M_0 e^{-\frac{t}{T_2}}. \tag{11}$$

This is known as spin-spin relaxation because the decay to equilibrium is based off of the spins of neighboring nuclei. Because all nuclei in the sample have spin, the spin of neighboring nuclei produce local magnetic fields B_{local} for other neighboring nuclei. This causes the nuclei to experience a new field

$$B_0' = B_0 + B_{\text{local}},$$

which causes the decay to equilibrium to occur at a faster rate than simply due to spin-lattice interactions. As such, T_2 values are generally smaller than T_1 values for a given sample.

III. EXPERIMENTAL DESIGN

A. Experimental Apparatus

The apparatus used was a TeachSpin PS1-A NMR spectrometer. The apparatus consists of a sample chamber, a control console, and an oscilliscope.

The sample chamber is made of a small holder to place the sample vial in, a receiver coil, a transmitter coil, and two permenant magnets. As seen in Fig. 1, the receiver coil, transmitter coil, and two permenant magnets are all orthogonal to each other. The two permenant magnets are coaxial, with one having the south pole facing the sample and the other having the north pole facing the sample. There are wires connecting the sample chamber to the control panel to allow the control of the transmitted radiowaves and recording of the sample response. The receiver coil is wrapped around the sample tube while the transmitter coils are perpendicular to the axis of the tube, with coils sandwiching the sample tube. The sample tube was filled with at least 2 mL of sample, with the samples being glycerol and mineral oil.

The control console is divided into three modules: the 15 MHz receiver, the pulse programmer, and the compound oscillator, amplifier, and mixer. The receiver is

connected to the receiver coil from the sample chamber to receive and amplify the radio frequency induced EMF from the sample. The pulse programer is used to generate the pulses used in the experiments. It is able to generate pulses ranging from 1 to 30 μs with the option of setting the delay time between two pulses to be 10 μs to 9.99 s. It is also possible to select repitition times for the pulse sequences from 1 ms to 10 s and the number of secondary pulses can be chosen from 0 to 99. The oscillator is a tunable 15 MHz oscillator that can be tuned by 1,000 Hz or 10 Hz.

The oscilloscope is connected to the mixer and the receiver to allow recording and visualization of the voltage output from both. It is through the oscilloscope that most observations in this experiment were made. Data was collected by reading from the oscilloscope.

Before beginning the experiments the following default setup should be used: place the sample vial into the sample chamber, turn on both the oscilloscope and the control console, the oscilloscope time scale set to 2.5 ms/box, the voltage scale for both mixer and receiver tuned to around 2.5 V/box and 1.5 V/box respectively, the receiver "Tuning" knob tuned to maximize the receiver reading on the oscilloscope, pulse programmer mode set to internal, repetition time set to 100 ms at 100%, synch A, A and B pulses both on, and the number of B pulses set to 1. The frequency on the oscillator is then tuned to around 15.53516 MHz for mineral oil and 15.53383 MHz for glycerol. However, the underlying goal of tuning the frequency is to tune it such that the mixer signal is a single peak that decays into a flat line.

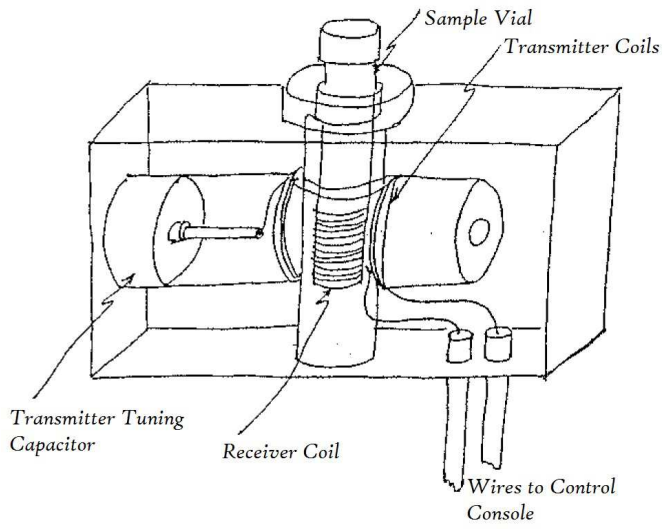

FIG. 1. The sample chamber of the NMR specrometer used. The main components are the receiver coil, the transmitter coil, and the two permenant magnets (not shown, but are coming in and out of the page).

B. Inversion Recovery Experiment to Determine T_1

First turn the "Pulse A Time Delay" knob to minimize the receiver reading while B pulse is turned off. Then turn on B pulse and tune "Pulse B Time Delay" so that it is approximately double the "Pulse A Time Delay" knob setting. Then, further tune "Pulse B Time Delay" knob to maximize the height of the peak observed in the receiver reading. This peak is known as a free induction decay (FID) and represents the magnetization of the sample in the direction of the receiver coil (denoted as the x axis) and it's subsequent decay back to equilibrium.

For the experiment set the delay time set to 1 ms. This is the first data point to record. The height of the peak in the receiver signal from the baseline is recorded with the delay time. The delay time is increased by 2 ms and the data recording continued. As the delay time is increased, the receiver signal peak should drop until no peak is seen. Great care should be taken to determine, with as high time resolution as possible, at what time delay the peak reaches zero height. The delay time is further increased, and the peak should grow again. The data collection is stopped at around 100 ms.

C. Spin Echo Experiment to Determine T_2

First turn the "Pulse A Time Delay" knob to maximize the receiver reading while B pulse is turned off. The reading to be maximized is the FID and should look like an exponentially decaying signal to the baseline. Make sure the delay time between A and B pulse is set to 1 ms. Then turn on B pulse and tune the "Pulse B Time Delay" so that a second peak is seen that looks like a small parabola growing out of the baseline. Tune the B time delay so that the size of the parabola is maximized. This parabola is known as the echo and arises because the π pulse causes the FID to reform and decay again. The height of the echo is recorded along with two times the time delay between A and B pulses. The time delay between A and B pulses is increased by 2 ms and the data recorded again. This is continued until the height of the echo cannot be resolved with good accuracy. The data collection generally stopped at around 30 ms and 50 ms time delay between A and B pulses for mineral oil and glycerol respectively.

IV. RESULTS

For all T_1 data, after collection, a plot was made of time delay from π-pulse to $\pi/2$-pulse in seconds versus arbitrary magnetization magnitude, which are shown in Fig. 2 and Fig. 3 for glycerol and mineral oil resspectively. When making this plot, all data before the magnitization reaches 0 is plotted as negative because only absolute values were recorded. This plot can be fit to

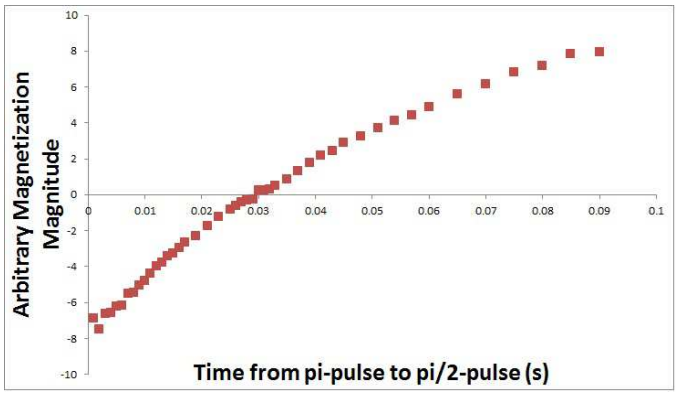

FIG. 2. Plot of the glycerol inversion recovery experiment data where T_1 was determined from the x-intercept of the graph.

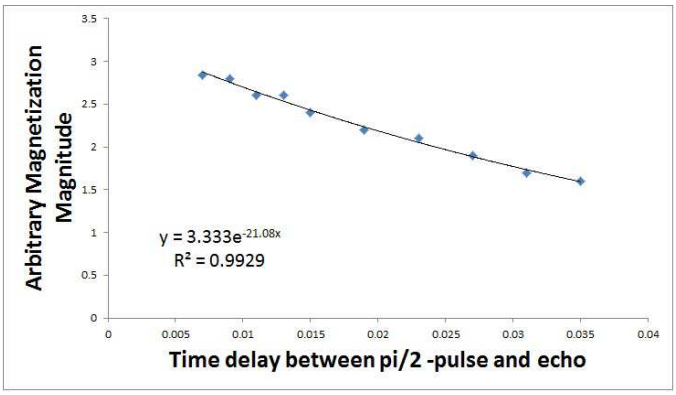

FIG. 4. Plot of the glyerol spin echo experiment data from which a trendline has been fitted. The equation for the trendline was used to determine T_2.

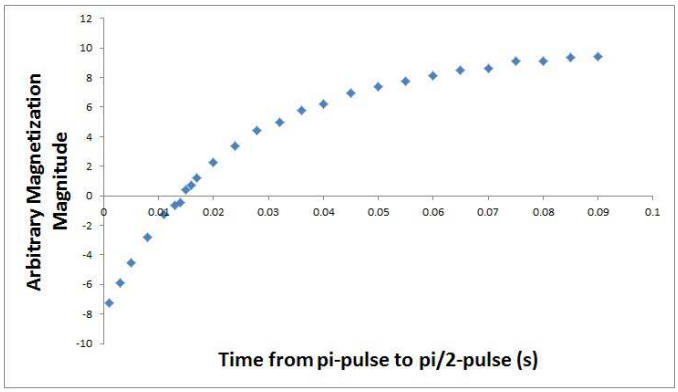

FIG. 3. Plot of the mineral oil inversion recovery experiment data where T_1 was determined from the x-intercept of the graph.

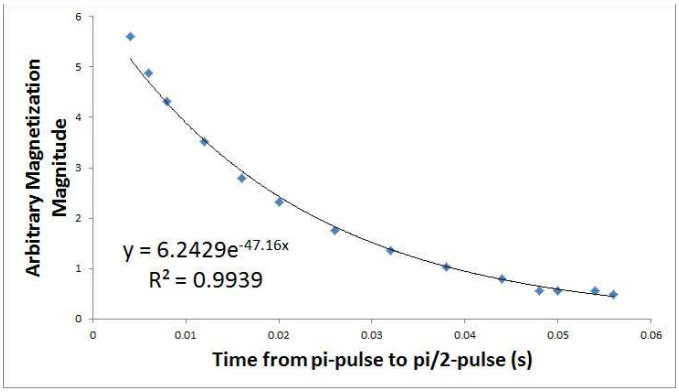

FIG. 5. Plot of the mineral oil spin echo experiment data from which a trendline has been fitted. The equation for the trendline was used to determine T_2.

a trend line, which could then be used to solve for T_1. Another method that can be used to solve for T_1, which is the method used in this paper, takes advantage of the relation

$$T_1 = \frac{t_n}{\ln(2)},$$

where t_n is the time delay from π-pulse to $\pi/2$-pulse, in seconds, where the arbitrary magnetization magnitude is zero. Through this method, it was discovered that, for glycerol, $T_1 = 42.5$ ms with an uncertainty of 1.7%. For mineral oil, it was discovered that $T_1 = 20.9$ ms with an uncertainty of 3.4%. The oscillator frequencies used for T_1 for glycerol and mineral oil were 15.53383 and 15.53516 MHz respectively.

For all the T_2 data, a plot was made of the time delay between the $\pi/2$-pulse and the echo, in seconds, versus arbitrary magnetization magnitude, which is shown in Fig. 4 and Fig. 5 for glycerol and mineral oil respectively. A best fit line was fit to the data, and the equation of that line found. The exponential term of the equation is in the form e^{at}. This exponential term can be equated to e^{-t/T_2} and T_2 can be found. Upon simplification, it was found that

$$T_2 = -\frac{1}{a}.$$

From this, we concluded that, for glycerol, $T_2 = 47.4$ ms with an uncertainty of 9.5%. For mineral oil, we found that $T_2 = 21.2$ ms with an uncertainty of 11.8%. The oscillator frequencies used for T_2 for glycerol and mineral oil were 15.53453 and 15.53563 MHz respectively.

V. DISCUSSION

For both glycerol and mineral oil, T_2 was found to be greater than T_1, which contradicts theory, which asserts that T_1 is greater than T_2, which is intriguing. While the sources for experimental error could not be found for why this is true, we believe that perhaps one area of improvement would be to try to reduce the uncertainty, which could be the underlying problem for this disconnect.

While our T_2 was found to be greater than T_1, which is unexpected, our data for mineral oil are within the

documented range for both T_1 and T_2, which range from 30-150 ms and 6-60 ms respectively [3]. Our data for glycerine for both T_1 and T_2 do not agree with documented data, which claim that the values are 87.5 and 58.0 ms respectively [4]. However, as neither of these sources were from peer reviewed journals, the data presented can only be used for comparison purposes.

Further experiments can be conducted with other samples. More interestingly, while tuning the oscillator for a resonant frequency, we found multiple resonant frequencies that worked for the samples we used. A meaningful next step could be to determine T_1 and T_2 for these frequencies also and compare the T_1 and T_2 values within the same molecule.

VI. ACKNOWLEDGEMENTS

We want to thank Dr. Gregory Severn for his time, patience, and help in troubleshooting and teaching the process and knowledge required to operate this lab.

[1] Melissinos, AC. Napolitano, J. *Experiments in Modern Physics*. Academic Pres, California, 2nd Edition, 2008.

[2] USD Physics Faculty. NMR Spin Echo Lab. *TeachSpin*, 2009.

[3] Wagner, EP. Understanding Precessional Frequency, Spin-Lattice and Spin-Spin Interactions in Pulsed Nuclear Magnetic Resonance Spectroscopy. *University of Pittsburgh Chem 1430 Manual*, 2012.

[4] Gibbs, ML. Nuclear Magnetic Resonance. *Georgia Institute of Technology Physics Lab Report*, 2007.